Published in final edited form as:
J Immunol. 2008 August 1; 181(3): 1978–1987.

Amyloid Precursor-like Protein 2 Increases the Endocytosis, Instability, and Turnover of the H2-K^d MHC Class I Molecule[1]

Amit Tuli[*,†], **Mahak Sharma**[*], **Mary M. McIlhaney**[†], **James E. Talmadge**[‡], **Naava Naslavsky**[*], **Steve Caplan**[*], and **Joyce C. Solheim**[2,*,†,‡]

[*]*Department of Biochemistry and Molecular Biology, University of Nebraska Medical Center, Omaha, NE, USA*

[†]*Eppley Institute for Research in Cancer and Allied Diseases, University of Nebraska Medical Center, Omaha, NE, USA*

[‡]*Department of Pathology and Microbiology, University of Nebraska Medical Center, Omaha, NE, USA*

Abstract

The defense against the invasion of viruses and tumors relies on the presentation of viral and tumor-derived peptides to cytotoxic T lymphocytes by cell surface major histocompatibility complex

[1]This work was supported by National Institutes of Health Grant GM57428 (to J.C.S.) and GM74876 (to S.C.), the Nebraska Research Initiative Program in Translational Biotechnology Research (to J.E.T. and J.C.S.), UNMC Graduate Studies Fellowships (to A.T. and M.S.), and a Nebraska Center for Cellular Signaling Fellowship (to M.S.). Core facilities at the University of Nebraska Medical Center receive support from the NIH Cancer Center Support Grant P30 CA036727.

[2]Address correspondence and reprint requests to Dr. Joyce C. Solheim, Eppley Institute for Research in Cancer and Allied Diseases, University of Nebraska Medical Center, 986805 Nebraska Medical Center, Omaha, NE, USA 68198-6805. Phone: (402) 559-4539, fax: (402) 559-4651, E-mail address: jsolheim@unmc.edu

[3]Abbreviations

APLP2 amyloid precursor-like protein 2

APP amyloid precursor protein

β_2m beta 2-microglobulin

CD99 Cluster of Differentiation 99

CHAPS 3-[(3-cholamidopropyl)dimethylammonio]-1-propanesulfonate

ER endoplasmic reticulum

TAP transporter associated with antigen processing

Disclosures
The authors have no financial conflict of interest.

(MHC) class I molecules. Previously, we showed that the ubiquitously expressed protein amyloid precursor-like protein 2 (APLP2) associates with the folded form of the MHC class I molecule K^d. In the current study, APLP2 was found to associate with folded K^d molecules following their endocytosis and to increase the amount of endocytosed K^d. In addition, increased expression of APLP2 was shown to decrease K^d surface expression and thermostability. Correspondingly, K^d thermostability and surface expression were increased by down-regulation of APLP2 expression. Overall, these data suggest that APLP2 modulates the stability and endocytosis of K^d molecules.

Keywords

antigen presentation/processing; cell surface molecules; MHC

Introduction

The presentation of antigenic peptides to T lymphocytes by major histocompatibility complex (MHC) molecules is essential for recognition and killing of infected and malignant cells. Assembly of MHC class I heavy chain with antigenic peptide and with the MHC class I light chain, beta 2-microglobulin (β_2m) occurs in the endoplasmic reticulum (ER). Peptide processing and loading of MHC class I molecules involves the participation of several ER proteins: the transporter associated with antigen processing (TAP), tapasin, calreticulin, ERp57, Bap 29/31, protein disulfide isomerase, and ER aminopeptidase (1-5). Evidence also indicates that there is regulation of MHC class I trafficking between the ER and the plasma membrane (2,6-11), although our understanding of this process is relatively limited.

A protein not restricted to the ER that associates with the MHC class I molecule is amyloid precursor-like protein 2 (APLP2) (12-14). APLP2 is a type I transmembrane protein which has a large ectodomain that can be cleaved off and secreted (15). APLP2 is ubiquitously expressed (15), and has a variety of cellular functions, i.e. involvement in mitotic segregation, neurite outgrowth, and epithelial cell migration (16-20). APLP2 is closely related in sequence to amyloid precursor protein (APP), but does not have a β-amyloid peptide domain (21-22).

APLP2 was first identified as a protein co-immunoprecipitating with H2-K^d by microsequencing and serological methods (12-13). We have found that transient transfection with APLP2-specific siRNA increases the cell surface expression of K^d, suggesting that normally APLP2 has a down-regulatory effect on K^d surface expression (14). Furthermore, APLP2 interacts with folded K^d molecules and not with open, peptide-free K^d molecules (14), and only associates with K^d in the presence of β_2m (13). Notably, APLP2 can be displaced from K^d in cell lysates by the addition of K^d-binding peptides (12), suggesting APLP2 interacts with the α1/α2 domain of K^d.

Our new studies have shown that increased expression of APLP2 reduces the quantity of K^d molecules present at the plasma membrane. We also demonstrated that increased APLP2 expression resulted in greater internalization and more rapid turnover of K^d. In addition, we found that APLP2 binds to the endocytosed K^d molecules. Furthermore, we found that the overall stability of K^d molecules is inversely related to the level of expression of APLP2 in the cell. These data indicate that APLP2 can interact with endocytosed K^d molecules and that it regulates the stability and surface expression of folded K^d molecules.

Materials and Methods

Antibodies

The 34-1-2 mAb recognizes the α1/α2 domain of K^d, D^d, and D^q, and it binds weakly to D^b and L^d but strongly to L^d associated with human β_2m and to some L^d mutants with amino acid substitutions in the peptide-binding groove (23-25). The 64-3-7 mAb can detect open, peptide-free L^d (26) and can also detect open forms of other MHC class I heavy chains, such as K^d, into which the 64-3-7 epitope has been introduced. Introduction of the 64-3-7 epitope does not impair peptide presentation, trafficking, or surface expression of K^d or other MHC class I molecules (27-30). The 30-5-7 mAb recognizes L^d molecules with a folded peptide-binding groove (26,31-34), and the 28-14-8 mAb binds to the α3 domain of L^d, D^b, D^q, and L^q (32, 33,35). The 34-1-2, 30-5-7, 28-14-8, and 64-3-7 Abs were donated by Dr. T. Hansen (Washington University, St. Louis, MO). The Ab used for APLP2 detection was made against full-length APLP2 (Calbiochem). The Ab recognizing β-actin (PanAb5) was purchased from Novus Biologicals.

Cell lines

Cell lines were grown in RPMI 1640 medium (Invitrogen) supplemented with 15% fetal bovine serum, glutamine, pyruvate and penicillin/streptomycin. The HeLa cell line was provided to us by Dr. W. Maury (University of Iowa, Iowa City, IA). HeLa cells were transfected with the cDNA encoding K^d with the 64-3-7 epitope (27) in the pIRIS.puro2 vector (BD Biosciences Clontech) or with an L^d cDNA (33) in the RSV.5neo vector (36). As mentioned above, previous studies have established the epitope-tagged K^d (etK^d) molecule as exhibiting normal assembly, folding, and trafficking (27). Selection in medium containing puromycin was performed to generate the stable HeLa-etK^d cell line. APLP2 siRNA and FLAG-tagged APLP2 constructs were generated for this study. The C-terminally FLAG-tagged APLP2 cDNA in the pCMVTag4A vector (Stratagene) was transfected into HeLa-etK^d cells to generate HeLa-etK^d cells expressing APLP2 at an elevated level. APLP2-specific short interfering RNA (siRNA) or inverse siRNA (the reverse sequence of the APLP2 siRNA) in the pSUPER vector was transfected into HeLa-etK^d cells to generate the stable HeLa-etK^d-APLP2 siRNA or HeLa-etK^d-inverse siRNA cell line, respectively. The sequence used for APLP2 siRNA was confirmed to be unique by search of the National Center for Biotechnology Information internet site. Stable clones expressing transfected APLP2, APLP2-specific siRNA, or APLP2 inverse siRNA were selected by incubation of the cells in medium with G418. Quantitative RT-PCR on samples from cells expressing APLP2-specific siRNA or inverse siRNA confirmed that APLP2-specific siRNA did not induce interferon expression more than the control inverse siRNA (data not shown). Western blotting for etK^d was used to select for stable transfectants that expressed the same level of etK^d. Transient transfection of FLAG-tagged APLP2 was done with analysis of the cells at 24 h following the transfection procedure. A transferrin receptor cDNA (37) expressing a C-terminal GFP tag in the Clontech EGFP vector (a gift from Dr. R. Lodge, Université du Quebec, Montréal, Quebec) was transiently transfected into HeLa-etK^d cells and confocal analysis was performed at 24 hours after transfection and flow cytometric analysis was performed at 48 hours after transfection. GFP-tagged Rab5 and Rab5Q79L cDNAs (38) in the EGFP vector (Clontech) were also generous gifts from Dr. R. Lodge. The Rab5 or Rab5Q79L construct was transiently transfected into HeLa-etK^d cells and confocal analysis was performed at 24 hours after transfection. All transfections were performed using Effectene (Qiagen) with 1 μg DNA per 0.5×10^6 cells.

Immunoprecipitations and Western blots

Immunoprecipitations and Western blotting were performed by a method similar to a published protocol (39). For protein immunoprecipitations, the cells were washed in PBS containing 20 mM iodoacetamide (Sigma-Aldrich) three times and lysed in 3-[(3-cholamidopropyl)

dimethylammonio]-1-propanesulfonate (CHAPS) lysis buffer. The CHAPS buffer contained 1% CHAPs (Roche Applied Science, Indianapolis, IN) in Tris-buffered saline (pH 7.4) with freshly added 0.2 mM PMSF and 20 mM iodoacetamide and a saturating amount of mAb. After 1 h on ice, the lysates were centrifuged to remove cell nuclei and incubated with Protein A-Sepharose beads (GE Healthcare Biosciences). The beads were washed in 0.1% CHAPS/20 mM IAA in TBS (pH 7.4) four times and boiled in 0.125 M Tris (pH 6.8)/2% SDS/12% glycerol/0.02% bromphenol blue to elute the proteins.

The eluted immunoprecipitates were electrophoresed on SDS-PAGE gels (Invitrogen) and transferred to Immobilon-P membranes (Millipore) for Western blots. After overnight blocking in reconstituted dry milk, membranes were incubated in diluted Ab for 2 h, washed three times with 0.05% Tween 20/PBS, and incubated for 1 h in a dilution of biotin-conjugated goat anti-mouse or anti-rabbit IgG (Caltag Laboratories). After three 0.05% Tween 20/PBS washes, the membranes were incubated with diluted streptavidin-conjugated horseradish peroxidase (Zymed) for 1 h, washed with 0.3% Tween 20/PBS three times, and incubated with enhanced chemiluminescence Western blot developing reagents (GE Healthcare Biosciences). The membranes were exposed to Kodak BioMax film (Eastman Kodak Co., Rochester, NY).

When Western blots were performed on cell lysates without an immunoprecipitation step, the cells were washed in PBS containing 20 mM iodoacetamide (Sigma-Aldrich) three times and lysed in buffer containing 0.125M Tris (pH 6.8)/2% (w/v) SDS/12% (v/v) glycerol/0.02% (w/v) bromophenol blue and fresh 0.2 mM PMSF. The lysates were incubated 1 h on ice, then centrifuged to pellet nuclear material. Samples of the supernatants were boiled before loading onto gels. Subsequent steps were performed as described above.

For the endoglycosidase (Endo) H assay, immunoprecipitations were first performed as described above, except proteins were eluted from the Protein A-Sepharose beads by boiling the samples for 5 min in 25 mM Tris (pH 8.3)/0.2 M glycine/0.1% SDS), centrifuging, and transferring the supernatants to fresh tubes. A 10X glycoprotein denaturing buffer (New England Biolabs) was added to 9 μl of supernatant to a final concentration of 1X, and the sample was boiled for 10 min. The sample was then split in half, and the reaction volume of each half was increased by addition of 2 μl of 10 G5 reaction buffer (New England Biolabs), 2 μl of Endo H (New England Biolabs) or 2 μl water, for the mock digestion), and a quantity of water sufficient to yield a final volume of 20 μl. The tubes were incubated for 1 h at 37°C, and then 5 μl of 0.5 M Tris (pH 6.8)/8% SDS/48% glycerol/0.08% bromophenol blue/8% β-mercaptoethanol were added. Samples were electrophoresed on 4-20% acrylamide Tris-glycine gels, and Western blots were performed as described above.

Assessment of the K^d turnover rate

For analysis of K^d turnover, a method that was previously described was used (40). Cells were treated with 10 μg/ml cycloheximide and then harvested at 0, 1, 2, 4, or 8 hours. Equivalent numbers of live cells were processed as described above for Western blots, and Ab 64-3-7 was used to detect the epitope-tagged K^d. Band intensity for K^d was normalized to β-actin band intensity at the same time point. Values were expressed as the percentage of remaining K^d at the 0, 1, 2, 4, or 8 hour time point.

Monitoring for induction of stress response

To test whether an increase in expression of APLP2 causes a cellular stress response, we monitored the expression of ER stress proteins, using a published approach (41). For this experiment, we used HeLa-etK^d cells (stably expressing K^d) that had been transiently transfected with APLP2-FLAG, transfected with vector only, or were left untransfected with either APLP2 or vector. At 32 h post-transfection, the medium was removed and fresh complete

medium was added and the cells were incubated for another 16 h. To generate a positive control, during the 16 h, HeLa-etK^d cells were treated with 2 μg/ml tunicamycin (Sigma-Aldrich). The samples were electrophoresed on 4-20% Tris-glycine acrylamide gels, transferred to blotting membranes, and Western blots of lysates of these cells were probed with an Ab specific for the KDEL sequence (Stressgen) present on the stress proteins GrP94 and BiP.

Biochemical analysis of the binding of APLP2 to endocytosed K^d

To demonstrate that APLP2 was bound to endocytosed K^d, HeLa-etK^d cells transiently transfected for 24 h with APLP2-FLAG were incubated with 34-1-2 Ab on ice for 20 min and then warmed at 37°C for 20 min. Any 34-1-2 Ab still bound to cell surface K^d was removed by washing with stripping buffer (0.5% acetic acid, 500 mM NaCl), and the cells were lysed. After centrifugation, Protein A-Sepharose was added to the lysate supernatant. Several controls were included in the experiment: lysed HeLa-etK^d cells, with no Ab added before or after lysis; HeLa and HeLa-etK^d cells lysed with 34-1-2 or with the 28-14-8 mAb (as an isotype control) in the lysis buffer; and HeLa-etK^d cells transiently transfected with APLP2-FLAG and treated with the surface-labeling procedure as described above for HeLa-etK^d except that an isotype control Ab (28-14-8) was used instead of 34-1-2. The samples were electrophoresed on 4→20% acrylamide Tris-glycine gels and transferred to blotting membranes, which were probed with mAb 64-3-7 to identify etK^d or with rabbit antiserum to identify co-precipitated APLP2.

Thermostability assays

The thermostability assay procedure used in this study was designed based on a published procedure (42). For the thermostability assay, cells were washed and lysed with CHAPS buffer and lysates were centrifuged to remove cell nuclei just as described in the section above. Aliquots from the supernatants were incubated at varied temperatures for 12 min on ice or in a Biometra T3 gradient thermocycler (Whatman Biometra). After the thermocycler incubations, immunoprecipitations and Western blots were performed on the aliquots as described in the section above. The amount of K^d in Western blot bands was quantified by densitometry using a Storm (Molecular Dynamics). The relative percentage of folded K^d at each incubation temperature between 25°C and 50°C was calculated after setting the amount of folded K^d at 4°C as 100%.

Flow cytometry assays

In flow cytometry assays, cells were suspended at 5×10^6/ml in PBS with 0.2% BSA and 0.1% sodium azide. Cell suspension aliquots in volumes of 0.1 ml were distributed to the wells of a 96-well plate. The cells were incubated with excess mAb or with BSA/azide/PBS alone (as a control) at 4°C for 30 min, washed twice, and incubated with a PE-conjugated, Fc-specific F $(ab')_2$ portion of goat anti-mouse IgG (Jackson ImmunoResearch) at 4°C for 30 min. The cells were washed 3 times, resuspended in BSA/azide/PBS, and analyzed on a FACSCalibur flow cytometer (BD Biosciences). Statistical analyses were done with the Cell Quest software (BD Biosciences).

Immunofluorescence analysis

To assess APLP2 association with MHC molecules endocytosed from the plasma membrane, cells were grown on glass cover slips, in some cases transiently transfected with APLP2-FLAG using Effectene (Qiagen), and incubated with anti-K^d Ab 34-1-2 at 37°C to allow endocytosis of cell surface K^d and bound Ab. Any Ab still bound to cell surface K^d molecules was then removed by incubation in stripping buffer (0.5% acetic acid/500 mM NaCl) for 90 sec and the cells were fixed with 4% (vol/vol) paraformaldehyde in PBS for 10 min. Fixed cells were incubated with anti-FLAG or anti-APLP2 rabbit antiserum prepared in staining solution (0.2% saponin wt/vol/0.5% wt/vol bovine serum albumin/PBS) for 1 h at room temperature. After 3

PBS washes (5 min/wash), the cells were incubated with a fluorochrome-conjugated mixture of secondary Abs (Alexa Fluor 568 goat anti-rabbit Ab and Alexa Fluor 488 goat anti-mouse Ab) in staining solution for 30 min at room temperature. After 3 washes in PBS (5 min/wash), the cells were mounted for image analysis. For all immunofluorescence experiments, the images were obtained with a Zeiss LSM 5 Pascal confocal microscope, using a 63X 1.4 numerical aperture lens with appropriate filters.

To ascertain whether the vesicles in which internalized K^d molecules associated with endogenous APLP2 were endosomes, HeLa-K^d cells (stably expressing K^d) were transfected for 24 h with Rab5 or the constitutively active Rab5 mutant Q79L (both GFP-tagged), grown on cover slips, and incubated with anti-K^d Ab 34-1-2 at 37°C for 15 min to allow endocytosis of K^d. After 15 min, any 34-1-2 Ab still bound to cell surface K^d molecules was removed by incubation in stripping buffer for 90 sec so that the subsequent immunofluorescence analysis would focus only on the internalized K^d molecules. The cells were fixed with 4% (vol/vol) paraformaldehyde in PBS for 10 min and incubated with anti-APLP2 rabbit antiserum (prepared in saponin-containing staining solution) for 1 h at room temperature. After 3 PBS washes, the cells were incubated with a fluorochrome-conjugated mixture of secondary Abs (Alexa Fluor 568 goat anti-rabbit Ab and Alexa Fluor 405 goat anti-mouse Ab) in staining solution for 30 min at room temperature. After 3 washes in PBS (5 min/wash), the cells were mounted for image analysis.

Results

Co-localization of APLP2 with folded K^d molecules in endosomal vesicles

Previous studies from our laboratory suggested that APLP2 down regulated the cell surface expression of K^d (14). To investigate whether the effect of APLP2 on K^d might be mediated through an endocytic mechanism, we analyzed whether APLP2 co-localized with K^d molecules that had been endocytosed from the plasma membrane and with an endosomal marker. An Ab uptake assay was performed with an anti-K^d Ab, using HeLa cells stably transfected with K^d and transiently transfected with Rab5-GFP or Rab5Q79L-GFP. Rab5 is an endosomal protein, and Rab5Q79L is a GTP-locked, non-hydrolyzable Rab5 mutant that stimulates endosomal membrane fusion (38). Expression of Rab5Q79L results in the formation of enlarged early endosomes that are accessible to internalized cargo (38), facilitating co-localization analysis. In our assay, we incubated non-permeabilized cells with anti-K^d Ab 34-1-2 for 15 min at 37° C. After removal of non-internalized 34-1-2 Ab with an acid wash, the cells were permeabilized and stained with Ab against APLP2. Co-localization of endogenous APLP2, internalized K^d, and Rab 5-GFP (Figure 1A) or Rab5Q79L (Figure 1B) was noticeable in the endosomes. Thus, APLP2 co-localizes with K^d molecules that have been internalized from the cell surface and that are present within endosomal vesicles.

APLP2 increased K^d endocytosis

We also examined the kinetics of the interaction of endogenous APLP2 with K^d molecules endocytosed from the plasma membrane. Anti-K^d mAb 34-1-2 was added to label the cell surface K^d molecules on HeLa-etK^d cells (stably expressing K^d), and the cells were incubated for varied amounts of time (0, 10, 20, or 30 min) at 37°C to allow internalization of K^d. The cells were then permeabilized and incubated first with primary Ab against APLP2, washed, and incubated with secondary Abs recognizing the anti-K^d and anti-APLP2 Abs. The 0 min time point is shown as evidence of thorough stripping of non-internalized anti-K^d Ab (Figure 2). Co-localization of endogenous APLP2 and internalized K^d was apparent by 10 min, and could still be visualized at 20 and 30 min (Figure 2).

K^d was also co-localized with FLAG-tagged APLP2 (transiently expressed in HeLa-etK^d cells) after K^d internalization from the cell surface for 20 min (Figure 3A). Confocal z-sectioning was done to confirm that internalized K^d and APLP2-FLAG were present in the same endocytic vesicles, and not merely within overlaid ones (Figure 3B). Furthermore, we demonstrated that APLP2 was bound to endocytosed K^d molecules, as shown by isolation of internalized 34-1-2^+ K^d and demonstration of APLP2 co-immunoprecipitated with the endocytosed K^d (Figure 3C). In these experiments, 34-1-2 Ab was incubated with HeLa-etK^d cells transiently expressing APLP2-FLAG, the cells were warmed at 37°C for 20 min and then acid stripped and lysed, the samples were electrophoresed, and the 34-1-2-immunoprecipitated K^d and co-immunoprecipitated APLP2 were identified by Western blotting. These data provide biochemical evidence for the binding of endocytosed K^d to APLP2.

Notably, from these confocal studies it could be seen that increased expression of APLP2 resulted in greater endocytosis of K^d. As shown in Figure 3A, the K^d fluorescence in transiently APLP2-transfected cells (indicated by dashed lines) was greater than in the cells within the same field that were not transfected with APLP2. The graph shown in Figure 3D displays the mean fluorescence intensity of internalized K^d in cells transiently expressing increased (FLAG-tagged) APLP2 versus cells that only expressed endogenous APLP2 (Figure 3D). (The data shown in the graph are from the 20 minute point in the same K^d uptake assay for which confocal microscopy results are shown in Figure 3A.) Cells expressing the higher level of APLP2 had significantly more internalized K^d than did cells expressing endogenous levels of APLP2 (Figure 3D). These findings indicate that APLP2 not only associates with endocytosed K^d, it potentiates its endocytosis. In contrast, elevated APLP2 expression did not significantly increase endocytosis of a different mouse MHC class I molecule, L^d (Figures 4A and B). APLP2 binds L^d more weakly than K^d and and has significantly less effect on the surface expression of L^d than K^d (data not shown). The effect of APLP2 on K^d endocytosis was specific to the folded form of K^d; there was no increase in open (64-3-7^+) etK^d internalization when APLP2 was over expressed (Figure 4C). In addition, the effect on folded K^d endocytosis was not seen when a different protein (transferrin receptor) instead of APLP2 was over expressed in HeLa-K^d cells (Figure 4D).

Increased expression of APLP2 does not induce expression of stress proteins

To confirm that expression of an increased amount of APLP2 did not induce a cellular stress reaction, which could conceivably have secondary effects on K^d endocytosis, we examined whether an increase in APLP2 expression led to heightened expression of stress proteins. To assess the stress response, we examined the cellular levels of GrP94 and BiP following APLP2 over expression. These stress proteins share a carboxy-terminal amino acid sequence (KDEL) that restricts them to the ER, and therefore they can be detected by an anti-KDEL Ab. HeLa cells stably expressing K^d and untransfected with APLP2, transiently transfected with vector only, or transiently transfected with increased levels of APLP2 were used in these experiments, along with HeLa-etK^d cells that had been treated with tunicamycin to induce a stress response (as a positive control). Western blots of lysates of these cell lines were probed with an Ab against the amino acid sequence KDEL, and proteins of the appropriate size to be GrP94 and BiP were detected only for the tunicamycin-treated positive control (Figure 4E). Thus, increased expression of APLP2 does not induce expression of the stress proteins GrP94 and BiP.

Increased APLP2 expression decreases the quantity of K^d molecules on the plasma membrane

Flow cytometric analysis of cells with stably over expressed, as well as stably down regulated, APLP2 was performed to assess the ability of APLP2 to regulate the amount of K^d expressed at the cell surface. For these experiments, HeLa-etK^d cells stably expressing FLAG-tagged

APLP2 were generated, and the tagged APLP2's expression and ability to bind K^d were confirmed (Figure 5A). By Endo H assays, we determined that K^d co-immunoprecipitating with the transfected APLP2 included both mature (Endo H-resistant) and immature (Endo H-sensitive) forms (Figure 5B). Stable APLP2 siRNA transfectants were also created (Figure 5C). Over-expression of APLP2 following transfection of FLAG-tagged APLP2 reduced the amount of K^d present at the plasma membrane to about 60% of the normal level (Figure 5D). In contrast, HeLa-etK^d cells that over expressed the transferrin receptor had K^d expression levels at 99.6% of the normal level (data not shown). The converse was also true, in that stable APLP2 siRNA transfectants expressed an increased level of K^d at the plasma membrane (about 1.7 fold higher than the level of K^d on the control cell lines) (Figure 5E). These results indicate that the level of cellular expression of APLP2 influences the amount of folded K^d available at the cell surface.

K^d thermostability and turnover was affected by the level of APLP2

To monitor for changes in K^d stability when the APLP2 level was increased, lysates of HeLa-etK^d cells transfected with APLP2, with vector alone, or neither were incubated on ice or at 5°C temperature intervals between 25°C and 50°C. Following the incubations, folded K^d molecules were immunoprecipitated, visualized by probing the electrophoresed and transferred samples on a Western blot, and quantified by densitometry. The relative percentage of folded K^d at each incubation temperature (based on setting the amount of folded K^d at 4°C as 100%) was graphed. As shown in Figure 6A, in the presence of an increased level of APLP2 the stability of folded K^d molecules was reduced. We also performed the same type of experiment using lysates of HeLa-etK^d cells transfected with APLP2 siRNA, inverse siRNA, or vector only. The presence of APLP2 siRNA increased the stability of K^d molecules in the temperature range between 35°C and 50°C (Figure 6B). Furthermore, by treating cells expressing normal or increased levels of APLP2 with cycloheximide for varied periods of time, we demonstrated that increased APLP2 causes a rise in the rate of K^d turnover (Figure 7A). Likewise, by incubating cells transfected with APLP2 siRNA or control siRNA with cycloheximide, we found that a decrease in the cellular APLP2 level lowered the K^d turnover rate (Figure 7B). Together, these results indicate that APLP2 destabilizes K^d/peptide complexes and augments K^d turnover.

Discussion

We have demonstrated that APLP2 associates with MHC class I molecules following MHC class I endocytosis. In addition, we found that over-expression, as well as reduction, of APLP2 is capable of modulating MHC class I cell surface expression and stability. The finding that cells in which APLP2 is over expressed have decreased cell surface MHC class I expression has implications for infectious disease and cancer, in that up-regulation of APLP2 expression by viruses or tumors could potentially aid in escape from CTL surveillance.

Previous studies have provided some insight into the regulation of MHC class I molecules beyond the ER. Tapasin has been shown to regulate retrograde transport of unstable MHC class I molecules back from the Golgi into the ER (11,43). Spiliotis et al. demonstrated that the transport of MHC class I molecules from the ER to the Golgi is mediated by cargo receptors (8). It has also been shown that when MHC class I molecules are highly over-expressed (20-50 fold), the excess MHC class I molecules could successfully traffic as far as the trans-Golgi, but most of the molecules were degraded before reaching the plasma membrane (6). Furthermore, the Cluster of Differentiation 99 (CD99) protein (also known as MIC2) seems to be involved in MHC class I transport modulation beyond the ER, since it has been found that CD99-deficient cells have delayed transport of MHC class I molecules between the Golgi and the plasma membrane, resulting in Golgi accumulation of MHC molecules (9). All of these

findings suggest that the level of MHC class I expression at the plasma membrane is determined by a series of regulatory steps.

At the plasma membrane, MHC class I molecules have been shown to be associated with insulin receptors (44-50). MHC class I molecules were found to bring insulin receptors in proximity to each other, enhancing their autophosphorylation and phosphoinositide 3-kinase activation (50). Furthermore, when cells were insulin stimulated, MHC class I molecules were also demonstrated to be phosphorylated and associated with phosphoinositide 3-kinase (50). Since APLP2 can also undergo phosphorylation (51), the previous observations with insulin receptor and MHC class I raise the question of whether the interaction of APLP2 with MHC class I affects the phosphorylation of APLP2 or the MHC class I molecule.

APLP2 is known to affect many intracellular pathways through mechanisms which are as yet only poorly understood. Hence, it is conceivable that APLP2 may influence K^d expression and stability by modulating the action of chaperones in the MHC class I antigen pathway. In this context, possible stress responses that might be induced by APLP2 could be considered. However, our findings do not support any role for APLP2 in inducing stress responses, since our data indicate that increased expression of APLP2 does not up regulate expression of stress response markers (GrP94 and BiP).

In our study, APLP2 was found to be associated with folded K^d molecules endocytosed from the cell surface and to increase K^d endocytosis. APLP2, and the closely related protein APP, have been shown to interact with the high-affinity choline transporter, and APP has been demonstrated to facilitate endocytosis of this transporter, although whether APLP2 also facilitates its endocytosis was not examined (52). The association of APLP2 with K^d molecules endocytosed from the cell surface suggests APLP2 may influence K^d degradation and/or recycling. Our observation that increased APLP2 causes a rise in the turnover rate of K^d is consistent with APLP2 facilitating K^d degradation. Differing reports have suggested that MHC class I molecules may be internalized either via clathrin-coated pits (53) or in a clathrin-independent manner (54). A sequence within the cytoplasmic tail of MHC class I molecules has been shown to be required for their endocytosis (55). MHC class I molecules expressed by B lymphoblastoid cells are continually endocytosed and recycled to the cell surface (56). The mechanism of MHC class I recycling appears to involve the Eps15 homology domain-containing protein (EHD1). EHD1 induces the formation of tubules which contain internalized MHC class I molecules, and over expression of EHD1 up-regulates MHC class I recycling (57), whereas siRNA down regulation of EHD1 delays the rate of MHC class I recycling (58).

Because APLP2 can associate with folded MHC class I molecules after their endocytosis, it may destabilize MHC/peptide complexes within the endocytic compartment. Following endocytosis, proteins can undergo deglycosylation and degradation (59). Destabilization by APLP2 could facilitate MHC class I turnover, and perhaps also MHC class I re-binding of new peptides within the cell. Overall, our data support a model in which APLP2 binds to endocytosed K^d molecules and regulates K^d endocytosis and stability, thereby modulating K^d cell surface expression.

Note added in proof

During the revision and resubmission of this manuscript, a comparative analysis of the variation in APLP2 binding, colocalization, and effect among mouse MHC class I allotypes was reported (60).

Acknowledgments

We thank Dr. Ted Hansen and Dr. Wendy Maury for gifts of antibodies and cell lines, Dr. Robert Lodge for gifts of DNA constructs, and Dr. Kay-Uwe Wagner for assistance with the thermocycler. We also gratefully acknowledge the assistance of Haley Capek, Vivek Gautam, Daniel McDermott, Miriam Menezes, and Phon T. Nguyen, and the personnel of the University of Nebraska Medical Center Cell Analysis Facility, Monoclonal Antibody Facility, and Molecular Biology Facility.

References

1. Cresswell P, Bangia N, Dick T, Diedrich G. The nature of the MHC class I peptide loading complex. Immunol. Rev 1999;172:21–28. [PubMed: 10631934]
2. Paquet ME, Cohen-Doyle M, Shore GC, Williams DB. Bap29/31 influences the intracellular traffic of MHC class I molecules. J. Immunol 2004;172:7548–7555. [PubMed: 15187134]
3. Park B, Lee S, Kim E, Cho K, Riddell SR, Cho S, Ahn K. Redox regulation facilitates optimal peptide selection by MHC class I during antigen processing. Cell 2006;127:369–382. [PubMed: 17055437]
4. Serwold T, Gonzalez F, Kim J, Jacon R, Shastri N. ERAAP customizes peptides for MHC class I molecules in the endoplasmic reticulum. Nature 2002;419:480–483. [PubMed: 12368856]
5. Saric T, Chang SC, Hattori A, York IA, Markant S, Rock KL, Tsujimoto M, Goldberg AL. An IFN-γ-induced aminopeptidase in the ER, ERAP1, trims precursors to MHC class I-presented peptides. Nat. Immunol 2002;3:1169–1176. [PubMed: 12436109]
6. Joyce S. Traffic control of completely assembled MHC class I molecules beyond the endoplasmic reticulum. J. Mol. Biol 1997;266:993–1001. [PubMed: 9086276]
7. Marguet D, Spiliotis ET, Pentcheva T, Lebowitz M, Schneck J, Edidin M. Lateral diffusion of GFP-tagged $H2L^d$ molecules and of GFP-TAP1 reports on the assembly and retention of these molecules in the endoplasmic reticulum. Immunity 1999;11:231–240. [PubMed: 10485658]
8. Spiliotis ET, Manley H, Osorio M, Zuniga MC, Edidin M. Selective export of MHC class I molecules from the ER after their dissociation from TAP. Immunity 2000;13:841–851. [PubMed: 11163199]
9. Sohn HW, Shin YK, Lee IS, Bae YM, Suh YH, Kim MK, Kim TJ, Jung KC, Park WS, Park C-S, Chung DH, Ahn K, Kim IS, Ko YH, Bang YJ, Kim CW, Park SH. CD99 regulates the transport of MHC class I molecules from the Golgi complex to the cell surface. J. Immunol 2001;166:787–794. [PubMed: 11145651]
10. Pencheva T, Edidin M. Clustering of peptide-loaded MHC class I molecules for endoplasmic reticulum export imaged by fluorescence resonance energy transfer. J. Immunol 2001;166:6625–6632. [PubMed: 11359816]
11. Paulsson KM, Kleijmeer MJ, Griffith J, Jevon M, Chen S, Anderson PO, Sjogren HO, Li S, Wang P. Association of tapasin and COPI provides a mechanism for the retrograde transport of major histocompatibility complex (MHC) class I molecules from the Golgi complex to the endoplasmic reticulum. J. Biol. Chem 2002;277:18266–18271. [PubMed: 11884415]
12. Feuerbach D, Burgert H-G. Novel proteins associated with MHC class I antigens in cells expressing adenovirus protein E3/19K. EMBO J 1993;12:3153–3161. [PubMed: 8344254]
13. Sester M, Feuerbach D, Frank R, Preckel T, Gutermann A, Burgert H-G. The amyloid precursor-like protein 2 associates with the major histocompatibility complex class I molecule K^d. J. Biol. Chem 2000;275:3645–3654. [PubMed: 10652361]
14. Morris CR, Petersen JL, Vargas SE, Turnquist HR, McIlhaney MM, Sanderson SD, Bruder JT, Yu YYL, Burgert H-G, Solheim JC. The amyloid precursor-like protein 2 and the adenoviral E3/19K protein both bind to a conformational site on $H\text{-}2K^d$ and regulate $H\text{-}2K^d$ expression. J. Biol. Chem 2003;278:12618–12623. [PubMed: 12506118]
15. Slunt HH, Thinakaran G, Von Koch C, Lo ACY, Tanzi RE, Sisodia SS. Expression of a ubiquitous, cross-reactive homologue of the mouse β-amyloid precursor protein. J. Biol. Chem 1994;269:2637–2644. [PubMed: 8300594]
16. Thinakaran G, Kitt CA, Roskams AJ, Slunt HH, Masliah E, von Koch C, Ginsberg SD, Ronnett GV, Reed RR, Price DL. Distribution of an APP homolog, APLP2, in the mouse olfactory system: a potential role for APLP2 in axogenesis. J. Neurosci 1995;15:6314–6326. [PubMed: 7472397]

17. Rassoulzadegan M, Yang Y, Cuzin F. APLP2, a member of the Alzheimer precursor protein family, is required for correct genomic segregation in dividing mouse cells. EMBO J 1998;17:4647–4656. [PubMed: 9707424]
18. Guo J, Thinakaran G, Guo Y, Sisodia SS, Yu FX. A role for amyloid precursor-like protein 2 in corneal epithelial wound healing. Invest. Ophthalmol. Vis. Sci 1998;39:292–300. [PubMed: 9477985]
19. Cappai R, Mok SS, Galatis D, Tucker DF, Henry A, Beyreuther K, Small DH, Masters CL. Recombinant human amyloid precursor-like protein 2 (APLP2) expressed in the yeast *Pichia pastoris* can stimulate neurite outgrowth. FEBS Lett 1999;442:95–98. [PubMed: 9923612]
20. Li XF, Thinakaran G, Sisodia SS, Yu FS. Amyloid precursor-like protein 2 promotes cell migration toward fibronectin and collagen IV. J. Biol. Chem 1999;274:27249–27256. [PubMed: 10480944]
21. Glenner GG, Wong CW. Alzheimer's disease: initial report of the purification and characterization of a novel cerebrovascular amyloid. Biochem. Biophys. Res. Commun 1984;120:885–890. [PubMed: 6375662]
22. Masters CL, Simms G, Weinman NA, Multhaup G, McDonald BL, Beyreuther K. Amyloid plaque core protein in Alzheimer disease and Down syndrome. Proc. Natl. Acad. Sci. USA 1985;82:4245–4249. [PubMed: 3159021]
23. Ozato K, Evans GA, Shykind B, Margulies D, Seidman JG. Hybrid H-2 histocompatibility gene products assign domains recognized by alloreactive T cells. Proc. Natl. Acad. Sci. USA 1983;80:2040–2043. [PubMed: 6188160]
24. Nieto M, Song ES, McKinney D, McMillan MM, Goodenow RS. The association of H-2Ld with human beta-2 microglobulin induces localized conformational changes in the alpha-1 and -2 superdomain. Immunogenetics 1989;30:361–369. [PubMed: 2478461]
25. Solheim JC, Carreno BM, Myers NB, Lee DR, Hansen TH. Peptide-induced rescue of serologic epitopes on class I MHC molecules. J Immunol 1995;154:1188–1197. [PubMed: 7529793]
26. Smith JD, Myers NB, Gorka J, Hansen TH. Model for the in vivo assembly of nascent L^d class I molecules and for the expression of unfolded L^d molecules at the cell surface. J. Exp. Med 1993;178:2035–2046. [PubMed: 8245780]
27. Yu YYL, Myers NB, Hilbert CH, Harris MR, Balendiran GK, Hansen THTH. Definition and transfer of a serological epitope specific for peptide-empty forms of MHC class I. Int. Immunol 1999;11:1897–1906. [PubMed: 10590255]
28. Myers NB, Harris MR, Connolly JM, Lybarger L, Yu YY, Hansen TH. K^b, K^d, and L^d molecules share common tapasin dependencies as determined using a novel epitope tag. J. Immunol 2000;165:5656–5663. [PubMed: 11067922]
29. Harris MR, Lybarger L, Myers NB, Hilbert CC, Solheim JC, Hansen TH, Yu YY. Interactions of HLA-B27 with the peptide loading complex as revealed by heavy chain mutations. Int. Immunol 2001;13:1275–1282. [PubMed: 11581172]
30. Lybarger L, Yu YYL, Chun T, Wang C-R, Grandea AG III, Van Kaer L, Hansen TH. Tapasin enhances peptide-induced expression of H2-M3 molecules, but is not required for the retention of open conformers. J. Immunol 2001;167:2097–2105. [PubMed: 11489993]
31. Ozato K, Hansen TH, Sachs D. Monoclonal antibodies to mouse MHC antigens. II. Antibodies to the H-$2L^d$ antigen, the product of a third polymorphic locus of the mouse major histocompatibility complex. J. Immunol 1980;125:2473–2477. [PubMed: 7191868]
32. Evans GA, Margulies DH, Shykind B, Seidman JG, Ozato K. Exon shuffling: mapping polymorphic determinants on hybrid mouse transplantation antigens. Nature 1982;300:755–757. [PubMed: 6184620]
33. Solheim JC, Carreno BM, Smith JD, Gorka J, Myers NB, Wen Z, Martinko JM, Lee DR, Hansen TH. Binding of peptides lacking consensus anchor anchor residue alters H-$2L^d$ serologic recognition. J. Immunol 1993;151:5387–5397. [PubMed: 7693810]
34. Smith JD, Solheim JC, Carreno BM, Hansen TH. Characterization of class I MHC folding intermediates and their disparate interactions with peptide and β_2-microglobulin. Mol. Immunol 1995;32:531–540. [PubMed: 7783756]

35. Ozato K, Sachs DH. Monoclonal antibodies to mouse MHC antigens. III. Hybridoma antibodies reacting to antigens of the H-2^b haplotype reveal genetic control of isotype expression. J. Immunol 1981;126:317–321. [PubMed: 6935293]
36. Long EO, Rosen-Bronson S, Karp DR, Malnati M, Sekaly RP, Jaraquemada D. Efficient cDNA expression vectors for stable and transient expression of HLA-DR in transfected fibroblasts and lymphoid cells. Hum. Immunol 1991;31:229–235. [PubMed: 1655683]
37. Zerial M, Melancon P, Schneider C, Garoff H. The transmembrane segment of the human transferrin receptor functions as a signal peptide. EMBO J 1986;5:1543–1550. [PubMed: 3017701]
38. Stenmark H, Parton RG, Steele-Mortimer O, Lutcke A, Gruenberg J, Zerial M. Inhibition of rab5 GTPase activity stimulates membrane fusion in endocytosis. EMBO J 1994;13:1287–1296. [PubMed: 8137813]
39. Turnquist HR, Solheim JC. Analysis of MHC class I interactions with endoplasmic reticulum proteins. Methods Mol. Biol 2001;156:165–173. [PubMed: 11068758]
40. Rinderknecht CH, Belmares MP, Catanzarite TLW, Bankovich AJ, Holmes TH, Garcia KC, Nanda NK, Busch R, Kovats S, Mellins ED. Posttranslational regulation of I-E^d by affinity for CLIP. J. Immunol 2007;279:5907–5915. [PubMed: 17947664]
41. Sato T, Susuki S, Suico MA, Miyata M, Ando Y, Mizuguchi M, Takeuchi M, Dobashi M, Shuto T, Kai H. Endoplasmic reticulum quality control regulates the fate of transthyretin variants in the cells. EMBO J 2007;26:2501–2512. [PubMed: 17431395]
42. Williams AP, Peh CA, Purcell AW, McCluskey J, Elliott T. Optimization of the MHC class I peptide cargo is dependent on tapasin. Immunity 2002;16:509–520. [PubMed: 11970875]
43. Paulsson KM, Jevon M, Wang JW, Li S, Wang P. The double lysine motif of tapasin is a retrieval signal for retention of unstable MHC class I molecules in the endoplasmic reticulum. J. Immunol 2006;176:7482–7488. [PubMed: 16751394]
44. Fehlmann M, Chvatchko Y, Brandenburg D, van Obberghen E, Brossette N. The subunit structure of the insulin receptor and molecular interactions with the major histocompatibility complex antigens. Biochimie 1985;67:1155–1159. [PubMed: 2416352]
45. Fehlmann M, Peyron J-F, Samson MA, van Obberghen E, Brandenburg D, Brossette N. Molecular association between major histocompatibility complex class I antigens and insulin receptor in mouse liver membranes. Proc. Natl. Acad. Sci. USA 1985;82:8634–8637. [PubMed: 3866245]
46. Due C, Simonsen M, Olsson L. The major histocompatibility complex class I heavy chain as a structural subunit of the human cell membrane insulin receptor: implication for the range of biological functions of histocompatibility antigens. Proc. Natl. Acad. Sci. USA 1986;83:6007–6011. [PubMed: 3090548]
47. Phillips ML, Moule ML, Delovitch TL, Yip CC. Class I histocompatibility antigens and insulin receptors: evidence for interactions. Proc. Natl. Acad. Sci. USA 1986;83:3474–3478. [PubMed: 3010300]
48. Kittur D, Shimizu Y, DeMars R, Edidin M. Insulin binding to human B lymphoblasts is a function of HLA haplotype. Proc. Natl. Acad. Sci. USA 1987;84:1351–1355. [PubMed: 3547409]
49. Edidin M, Reiland J. Dynamic measurements of the associations between class I MHC antigens and insulin receptors. Mol. Immunol 1990;27:1313–1317. [PubMed: 2274061]
50. Ramalingam TS, Chakrabarti A, Edidin M. Interaction of class I human leukocyte antigens (HLA-I) molecules with insulin receptors and its effect on the insulin-signaling cascade. Mol. Biol. Cell 1997;8:2463–2474. [PubMed: 9398668]
51. Taru H, Suzuki T. Facilitation of stress-induced phosphorylation of beta-amyloid precursor protein family members by X11-like/Mint2 protein. J. Biol. Chem 2004;279:21628–21636. [PubMed: 14970211]
52. Wang B, Yang L, Wang Z, Zheng H. Amyloid precursor protein mediates presynaptic localization and activity of the high-affinity choline transporter. Proc. Natl. Acad. Sci. USA 2007;104:14140–14145. [PubMed: 17709753]
53. Dasgupta JD, Watkins S, Slayter H, Yunis EJ. Receptor-like nature of class I HLA: endocytosis via coated pits. J. Immunol 1988;141:2577–2580. [PubMed: 2902138]
54. Radhakrishna H, Donaldson JG. ADP-ribosylation factor 6 regulates a novel plasma membrane recycling pathway. J. Cell Biol 1997;139:49–61. [PubMed: 9314528]

55. Vega MA, Strominger JL. Constitutive endocytosis of HLA class I antigens requires a specific portion of the intracytoplasmic tail that shares structural features with other endocytosed molecules. Proc. Natl. Acad. Sci. USA 1989;86:2688–2692. [PubMed: 2495533]

56. Reid PA, Watts C. Cycling of cell-surface MHC glycoproteins through primaquine-sensitive intracellular compartments. Nature 1990;346:655–657. [PubMed: 2166918]

57. Caplan S, Naslavsky N, Hartnell LM, Lodge R, Polishchuk RS, Donaldson JG, Bonifacino JS. A tubular EHD1-containing compartment involved in the recycling of major histocompatibility complex class I molecules to the plasma membrane. EMBO J 2002;21:2557–2567. [PubMed: 12032069]

58. Naslavsky N, Boehm M, Backlund PS Jr, Caplan S. Rabenosyn-5 and EHD1 interact and sequentially regulate protein recycling to the plasma membrane. Mol. Biol. Cell 2004;15:2410–2422. [PubMed: 15020713]

59. Schmitt M, Grand-Perret T. Regulated turnover of a cell surface-associated pool of newly synthesized apolipoprotein E in HepG2 cells. J. Lipid Res 1999;40:39–49. [PubMed: 9869648]

60. Tuli A, Sharma M, Wang X, Naslavsky N, Caplan S, Solheim JC. Specificity of amyloid precursor-like protein 2 interactions with MHC class I molecules. Immunogenetics 2008;60:303–313. [PubMed: 18452037]

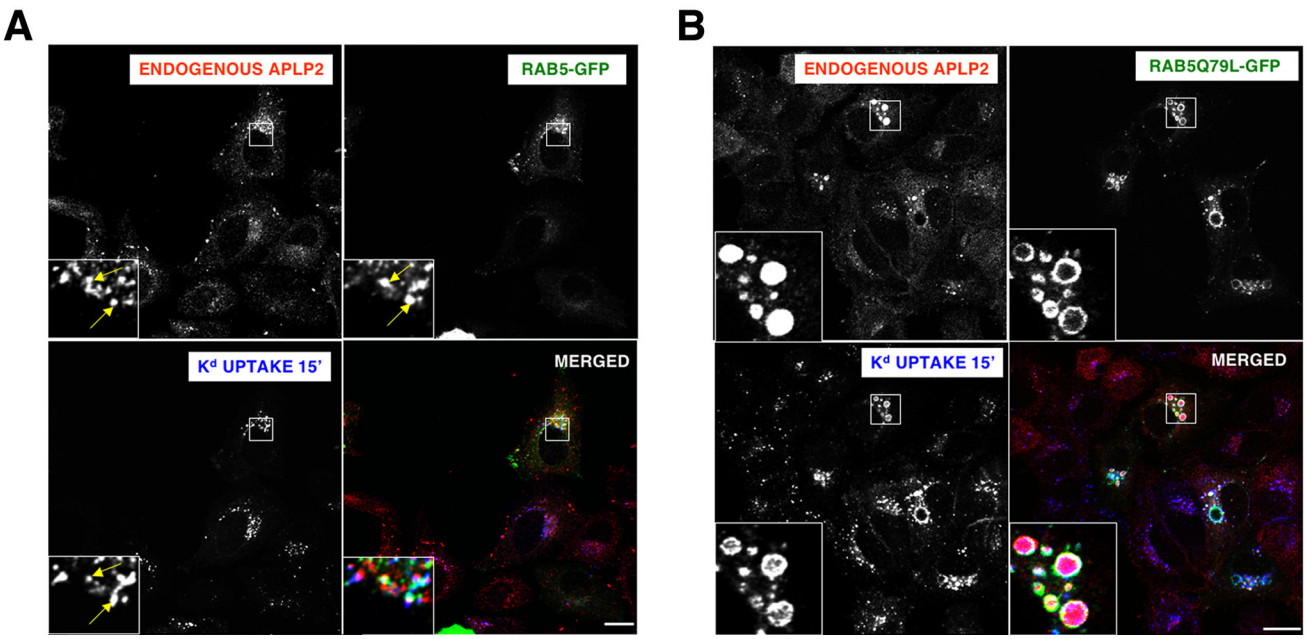

Figure 1.

Folded K^d molecules were co-localized with APLP2 in $Rab5^+$ early endosomes. (*A*) APLP2 and endocytosed K^d were co-localized with endosomal marker Rab5. (*B*) APLP2 and endocytosed K^d were co-localized with the Rab5 dominant negative mutant Rab5Q79L-GFP, which causes early endosomes to be enlarged. HeLa cells stably transfected with K^d and transfected with either Rab5 or Rab5Q79L-GFP were pulsed with anti-K^d Ab 34-1-2 and warmed for 15 min at 37°C. The cells were then incubated with 0.5% acetic acid/500 mM NaCl to strip non-internalized surface-bound 34-1-2 Ab. The cells were fixed with 4% paraformaldehyde, and incubated with rabbit anti-APLP2 serum in staining solution containing saponin, washed, and incubated with fluorescently labeled secondary antibodies in the same staining solution. The images were analyzed on a Zeiss LSM 5 Pascal confocal microscope. Red = APLP2; green = Rab5 or Rab5Q79L; blue = K^d; white = co-localized APLP2, K^d, and Rab5 or Rab5Q79L. Bar indicates 10 μm. Insets display more highly magnified images of the areas shown in the larger boxes, and the arrows in *A* indicate vesicles in which APLP2, Rab5, and K^d are co-localized.

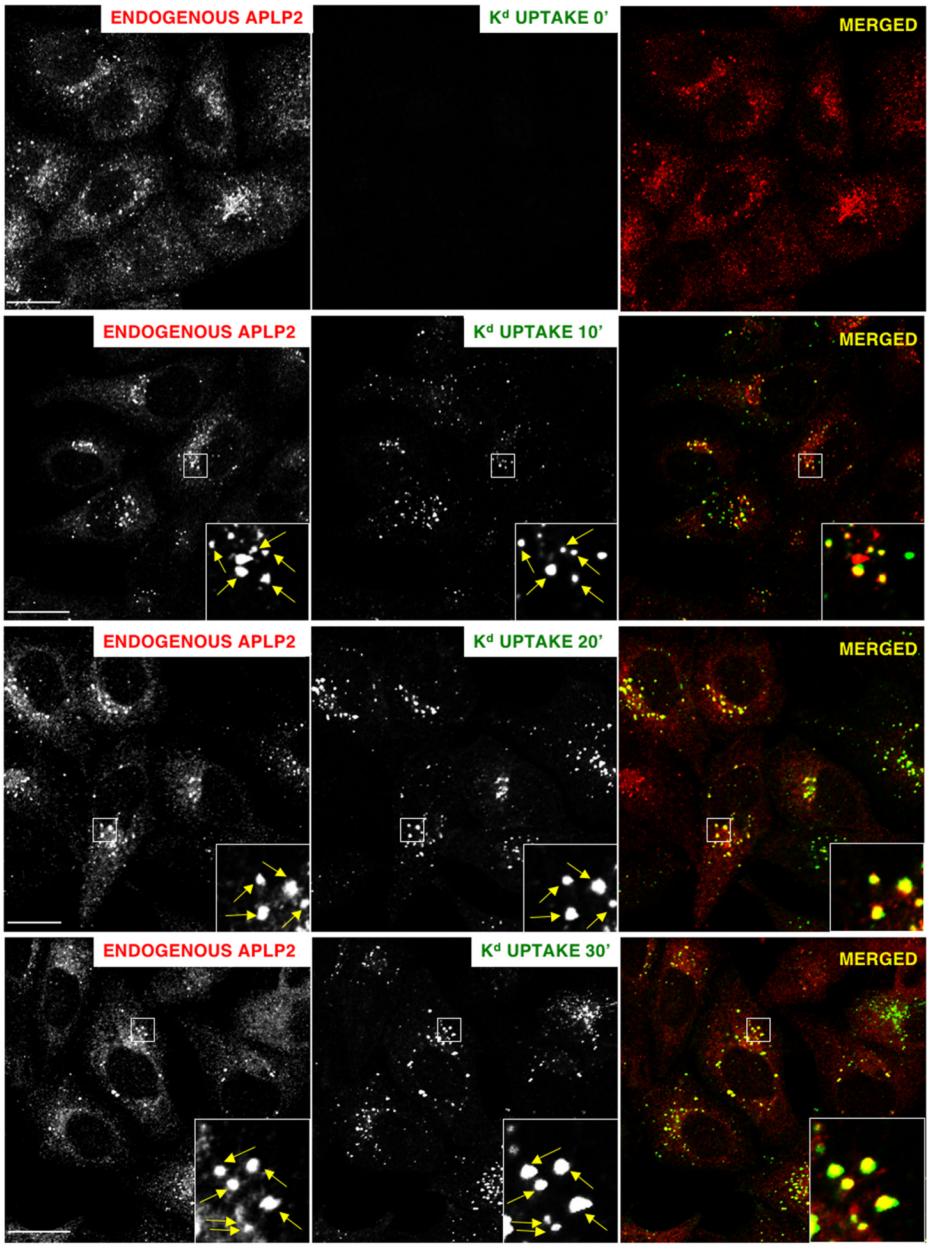

Figure 2.

Folded K^d molecules internalized from the cell surface could be found co-localized with endogenous APLP2 in vesicles at 10, 20, and 30 min after the start of anti-K^d Ab pulsing. HeLa cells stably transfected with K^d were incubated with anti-K^d Ab 34-1-2 for 0, 10, 20, or 30 min at 37°C. The cells were then treated with 0.5% acetic acid/500 mM NaCl to strip non-internalized surface-bound 34-1-2 Ab. The cells were fixed with 4% paraformaldehyde, and incubated with rabbit anti-APLP2 serum in staining solution containing saponin, washed, and incubated with fluorescently labeled secondary Abs in staining solution. Images were analyzed on a Zeiss LSM 5 Pascal confocal microscope. Red, APLP2; green, folded K^d; yellow, co-localized APLP2 and endocytosed K^d. Bar indicates 10 μm. For the 10, 20, and 30 min time

points, the insets depict more highly magnified images of the areas shown in the larger boxes, and the arrows in the insets indicate vesicles in which APLP2 and K^d are co-localized.

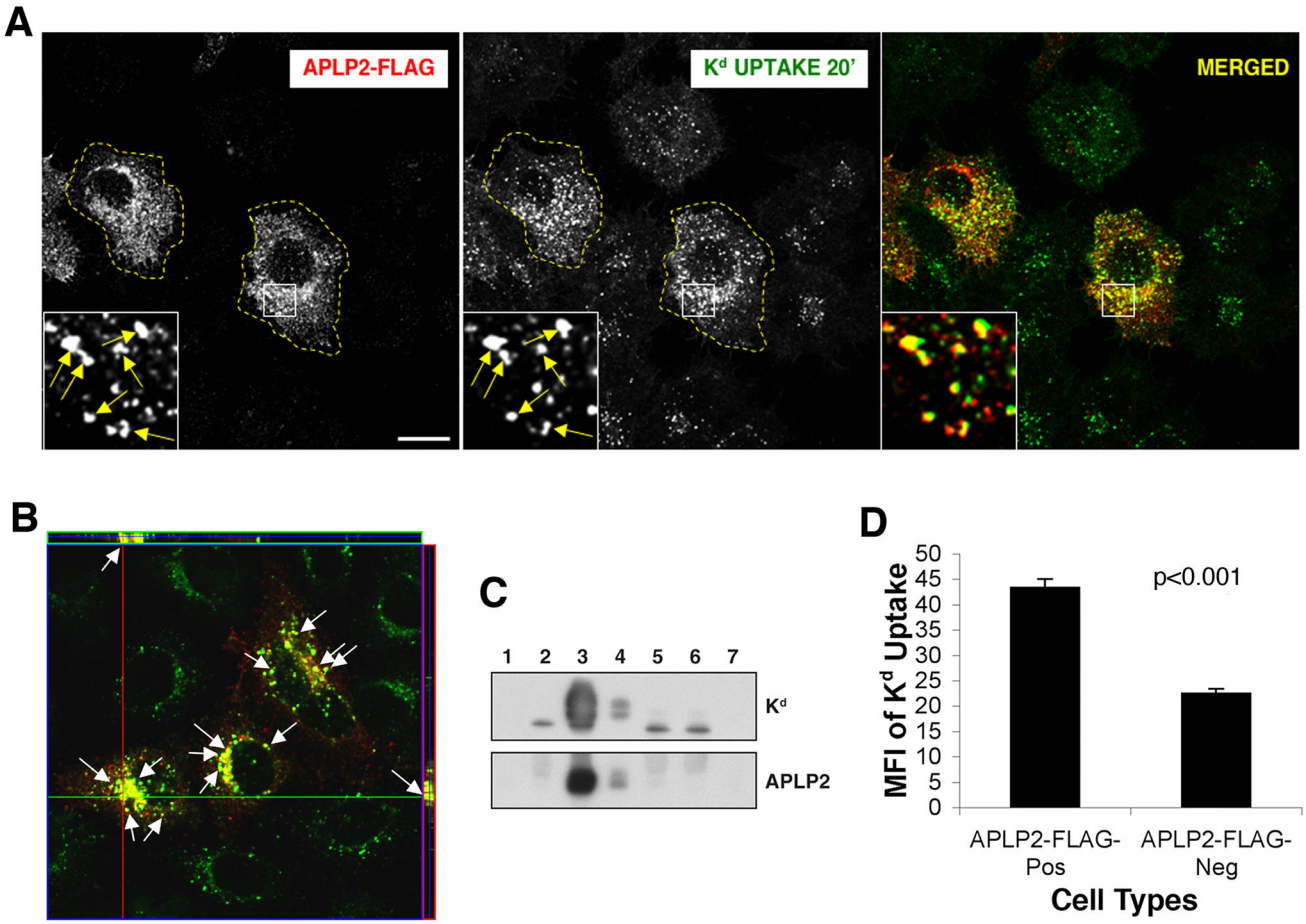

Figure 3.

Increased expression of APLP2 was found to enhance the endocytosis of K^d. (*A*) HeLa-etK^d cells (stably expressing K^d) were transiently transfected with APLP2-FLAG for 24 h. Anti-K^d Ab 34-1-2 was added and the cells were warmed to 37°C for 20 min. Following Ab internalization, the cells were treated with 0.5% acetic acid/500 mM NaCl to strip off non-internalized surface-bound 34-1-2. The cells were fixed with 4% paraformaldehyde, incubated in staining solution (containing saponin) with rabbit anti-FLAG, washed, and incubated in staining solution and fluorescently labeled secondary antibodies, and visualized with a Zeiss LSM 5 Pascal confocal microscope. Red, APLP2; green, folded K^d; yellow, co-localized APLP2 and K^d. Representative APLP2-transfected cells are outlined with a dashed line. Bar corresponds to 10 μm. The insets display more highly magnified images of the areas depicted in the larger boxes. Arrows in the insets point to vesicles in which APLP2-FLAG and K^d are co-localized. (*B*) Results confirming that APLP2 and endocytosed K^d are located together in vesicles were obtained by taking z-section images. Serial z-section images were acquired at 0.4 μm intervals of HeLa-etK^d cells transfected with APLP2-FLAG for 24 h, surface-labeled with 34-1-2 and incubated at 37°C for 15 min. The arrows point to common membrane structures on a representative photomicrograph. APLP2, red, K^d, green, and merged green and red, yellow. These data confirm that the indicated APLP2- and K^d-containing structures are the same endocytic vesicles and not overlaid vesicles. (*C*) APLP2 was bound to endocytosed K^d. *Lane 1*: Lysate of HeLa-etK^d cells plus Protein A-Sepharose beads; *Lanes 2 and 3*: 34-1-2 Ab was added to lysates of HeLa and HeLa-etK^d for immunoprecipitation of K^d; *Lane 4*: HeLa-etK^d cells transfected with APLP2-FLAG for 24 h were incubated with 34-1-2 Ab for 20 min

on ice and then transferred to 37°C for 20 min, non-internalized 34-1-2 Ab was removed by an acid wash, the cells were lysed and centrifuged, and Protein A-Sepharose was added to the lysate supernatant; *Lanes 5 and 6*: Isotype control Ab (28-14-8) was added to lysates of HeLa and HeLa-etK^d and an immunoprecipitation procedure was performed; *Lane 7*: HeLa-etK^d cells transfected with APLP2-FLAG for 24 h were incubated with the isotype control Ab 28-14-8 for 20 min on ice and then transferred to 37°C for 20 min, the cells were treated with an acid wash, lysed, and centrifuged, and Protein A-Sepharose was added to the lysate supernatant. The samples were electrophoresed on 4→20% acrylamide Tris-glycine gels, transferred to blots, and probed with mAb 64-3-7 that recognizes etK^d (*top panel*) or with rabbit antiserum against APLP2 (*bottom panel*). The bands in the 2nd, 5th, and 6th lanes are non-specific bands. (*D*) Higher expression of APLP2 resulted in increased K^d endocytosis. Image J Software (http://rsb.info.nih.gov) was used to measure the fluorescence of the internalized K^d expressed by >80 cells transfected with APLP2-FLAG and >80 cells not transfected with APLP2-FLAG within the experiment for which confocal data is shown in Figure 3A. Mean fluorescence intensities and standard errors of the mean were calculated, and p values were determined by the use of Student's paired t test.

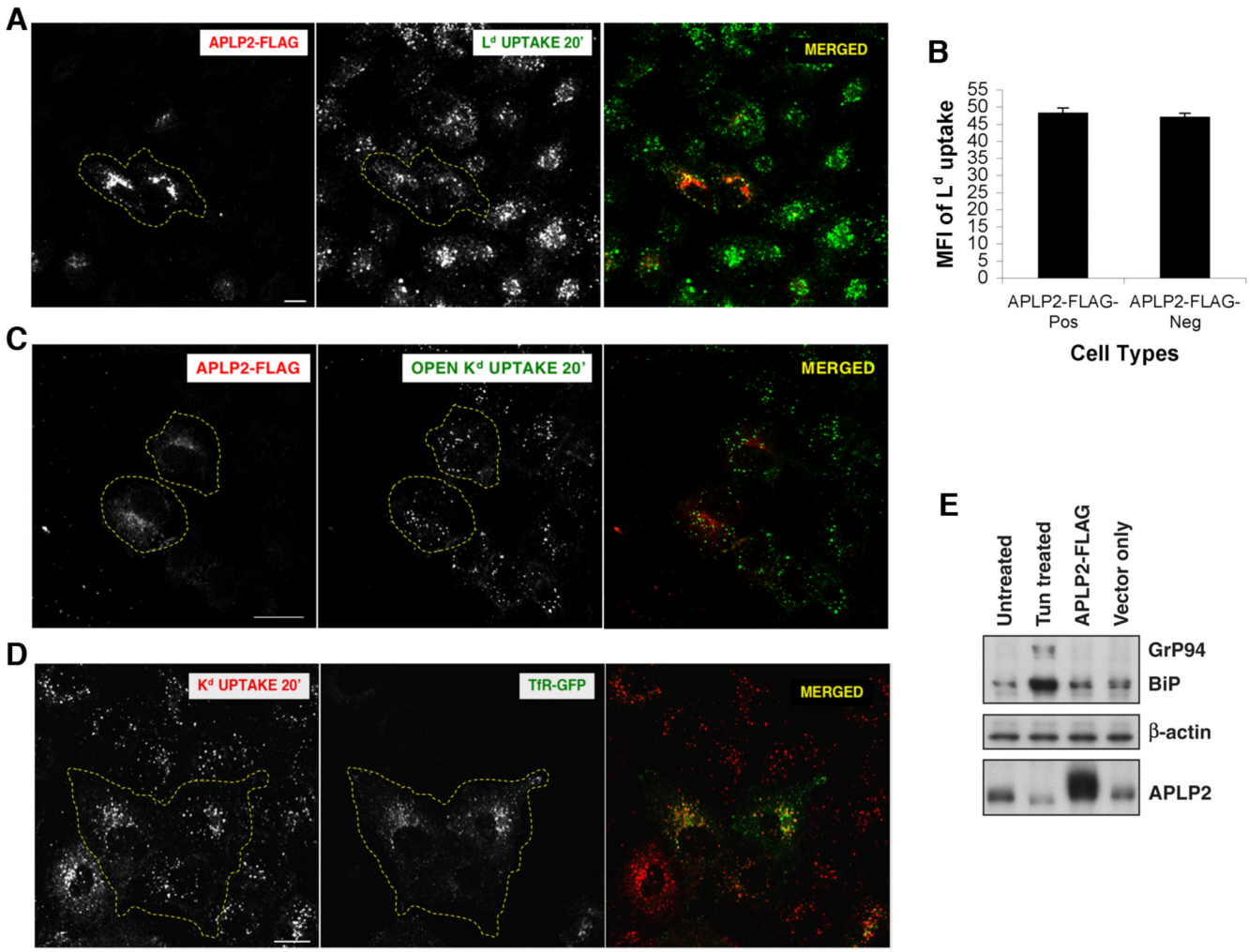

Figure 4.

(*A*) Increased expression of APLP2 did not enhance the endocytosis of folded L^d. The experiment was performed as described in the legend for Figure 3A, except that HeLa cells stably transfected with L^d were used instead of HeLa-etK^d cells, and 30-5-7 (an Ab that recognizes folded L^d molecules) was used instead of 34-1-2. The bar corresponds to 10 μm. (*B*) Quantification of confocal microscopy data demonstrating that higher expression of APLP2 did not increase L^d endocytosis. Image J Software (http://rsb.info.nih.gov) was used to measure the fluorescence of the internalized L^d expressed by >80 cells transfected with APLP2-FLAG and >80 cells not transfected with APLP2-FLAG within the experiment for which confocal data is shown in Figure 4A. Mean fluorescence intensities and standard errors of the mean were calculated, and p values were determined by the use of Student's paired t test. (*C*) Increased expression of APLP2 did not enhance the endocytosis of open K^d. The experiment was performed as described for Figure 3A, except that 64-3-7 was used instead of 34-1-2. Bar corresponds to 10 μm. (*D*) Increased expression of transferrin receptor did not enhance the endocytosis of folded K^d. The experiment was performed as described for Figure 3A, except that the cells were transiently transfected with GFP-tagged transferrin receptor (TfR-GFP) instead of APLP2-FLAG. Bar corresponds to 10 μm. (*E*) Increased expression of APLP2 does not up regulate expression of ER stress proteins. HeLa-etK^d cells (stably expressing K^d) were transfected with APLP2-FLAG, transfected with vector only, or were left untransfected.

APLP2-FLAG-transfected and Vector only-transfected cells were not treated with tunicamycin. Tunicamycin (2 μg/ml) was used to induce a stress response in HeLa-etK^d cells (lane labeled as "Tun treated") to create a positive control. The lane corresponding to cells untransfected with APLP2-FLAG or vector and not treated with tunicamycin is labeled as "Untreated". Western blots of lysates of these cells were probed with an Ab recognizing the KDEL sequence (present on the stress proteins GrP94 and BiP, *top panel*), an Ab recognizing β-actin (*middle panel*), or an Ab recognizing APLP2 (*bottom panel*).

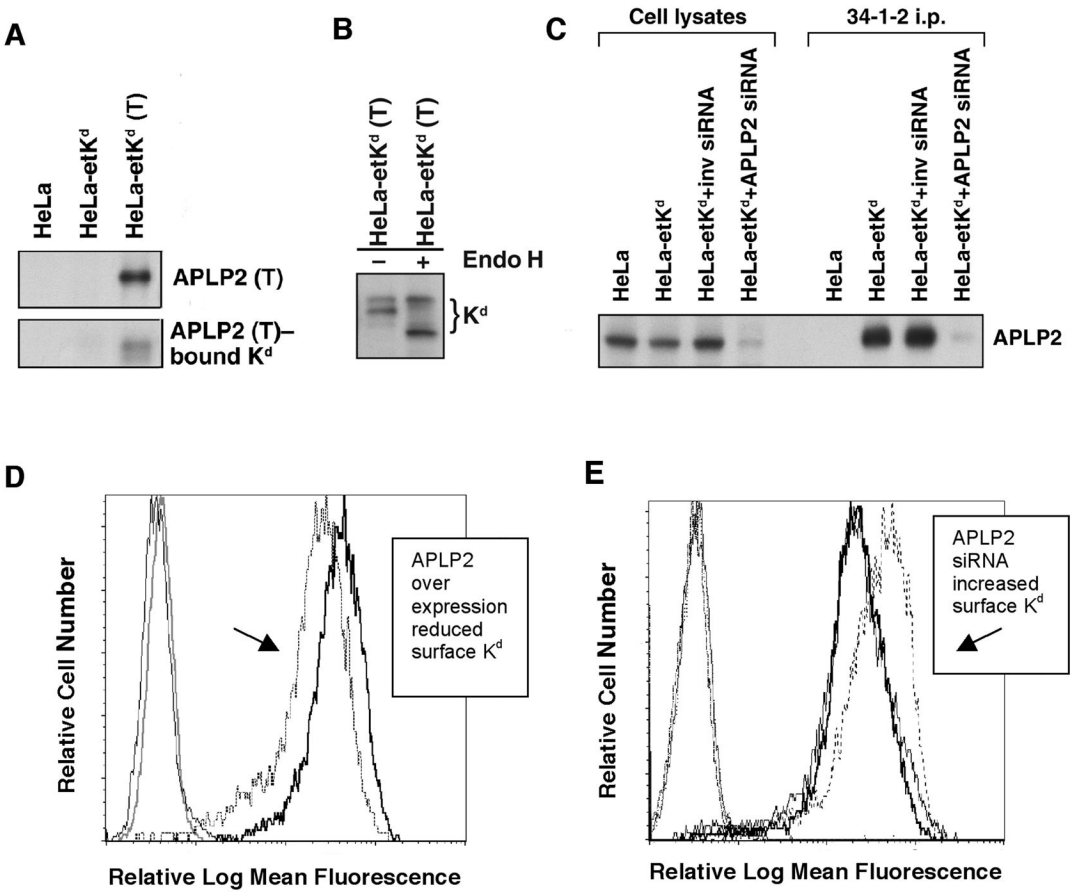

Figure 5.

The cell surface expression of K^d was affected when APLP2 expression was increased or decreased. (*A*) The expression of transfected, tagged APLP2 and the ability of tagged APLP2 to associate with K^d were verified. FLAG-tagged APLP2 [APLP2 (T)] was stably transfected into HeLa-etK^d cells (stably expressing K^d), and the APLP2-FLAG was immunoprecipitated with an anti-FLAG Ab from lysates of these HeLa-etK^d (T) cells. The immunoprecipitated proteins were electrophoresed, transferred to Western blots, and probed with Ab specific for APLP2 (*top panel*) or with an Ab that recognizes denatured epitope-tagged K^d (64-3-7) (*bottom panel*). HeLa and HeLa-etK^d-pCMV were used as negative controls. (*B*) The population of K^d molecules demonstrated to be bound to APLP2-FLAG included mature (Endo H-resistant) and immature (Endo H-sensitive) forms of K^d. APLP2-FLAG was immunoprecipitated with an anti-FLAG Ab from lysates of HeLa cells stably transfected with etK^d and transiently transfected with APLP2-FLAG (HeLa-etK^d (T) cells). Half of the immunoprecipitate was untreated (- Endo H), and half was incubated with Endo H (+ Endo H). Samples from each half were then electrophoresed on 4-20% acrylamide Tris-glycine gels, and Western blots of the electrophoresed samples were probed with an Ab that recognizes denatured epitope-tagged K^d (Ab 64-3-7). (*C*) Stable expression of APLP2 siRNA caused a down regulation of APLP2 expression and a resultant decrease in the amount of APLP2 associated with stably transfected K^d. A Western blot was probed with an Ab recognizing APLP2, revealing the levels of APLP2 in the indicated cell lysates and bound to K^d immunoprecipitated with 34-1-2. (*D*) Stably increased expression of APLP2 resulted in a decrease in stably transfected cell surface K^d

molecules. Thin solid line: HeLa-etK^d+pCMVTag4A with PE-conjugated secondary Ab (2°) only; medium solid line: HeLa-etK^d-APLP2 with 2°-PE; dashed line: HeLa-etK^d-APLP2 with anti-K^d Ab (34-1-2) and 2°-PE; thick solid line: HeLa-etK^d-pCMVTag4A with 34-1-2 and 2°-PE. (*E*) Stable down regulation of endogenous APLP2 expression caused an increase in the level of stably transfected K^d molecules at the plasma membrane. Thin solid line: HeLa-etK^d-pSuper1 with 2°-PE; dash-dot-dash line: HeLa-etK^d-APLP2 siRNA with 2°-PE; dotted line: HeLa-etK^d-APLP2 inverse siRNA (i.e., the reversed APLP2 siRNA sequence) with 2°-PE; medium line: HeLa-etK^d-pSuper1 with anti-K^d Ab (34-1-2) and 2°-PE; thick solid line: HeLa-etK^d-APLP2 inverse siRNA with 34-1-2 and 2°-PE; dashed line: HeLa-etK^d-APLP2 siRNA with 34-1-2 and 2°-PE.

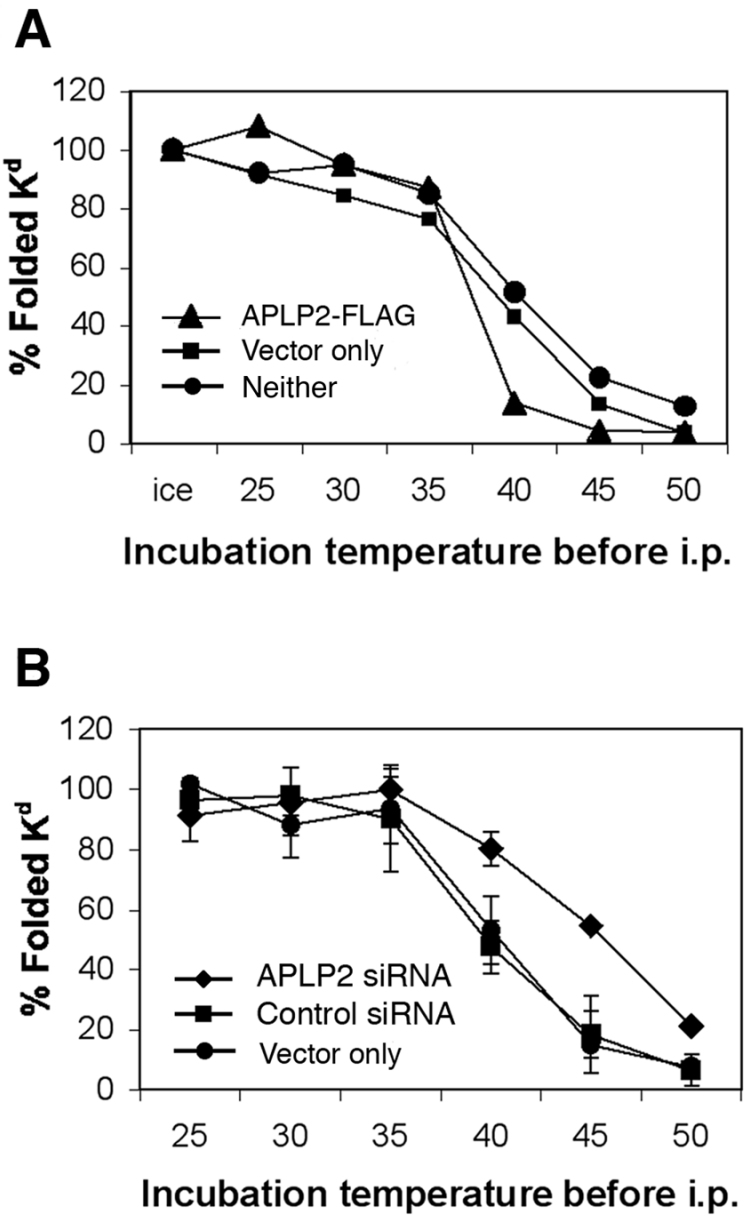

Figure 6.

Over expression of APLP2 decreased the stability of folded K^d molecules, and down regulation of APLP2 expression increased the stability of folded K^d molecules. Cell lysates were incubated for 12 minutes on ice or in a Biometra T3 gradient thermocycler (Whatman Biometra) at the indicated temperatures. After the thermocycler incubations, immunoprecipitations with anti-folded K^d Ab 34-1-2 were performed. The immunoprecipitates were electrophoresed and probed on a Western blot with Ab 64-3-7 to identify the tagged K^d heavy chain. Folded K^d was quantified by densitometry, and is presented on the graphs as the relative percentage of folded K^d at each incubation temperature after setting the amount of folded K^d at 4°C as 100%. (*A*) Increasing APLP2 expression by transfection of APLP2 into HeLa-etK^d cells decreased folded K^d stability. The results illustrated in the graph were obtained with HeLa-etK^d cells (stably expressing K^d) that had been stably transfected with FLAG-tagged APLP2 in the

pCMVTag4A vector ▲, with the pCMVTag4A vector alone ■, or with neither APLP2-pCMVTag4A nor pCMVTag4A ●). (*B*) Reduction of APLP2 expression by transfection of APLP2-siRNA into HeLa-etK^d cells improved folded K^d stability. The cells utilized were HeLa-etK^d cells (stably expressing K^d) that had been stably transfected with APLP2 siRNA in the pSuper vector ◆, with inverse siRNA (the reversed APLP2 siRNA sequence) in the pSuper vector ■, or the pSuper vector alone ●. Error bars represent the standard error of the mean.

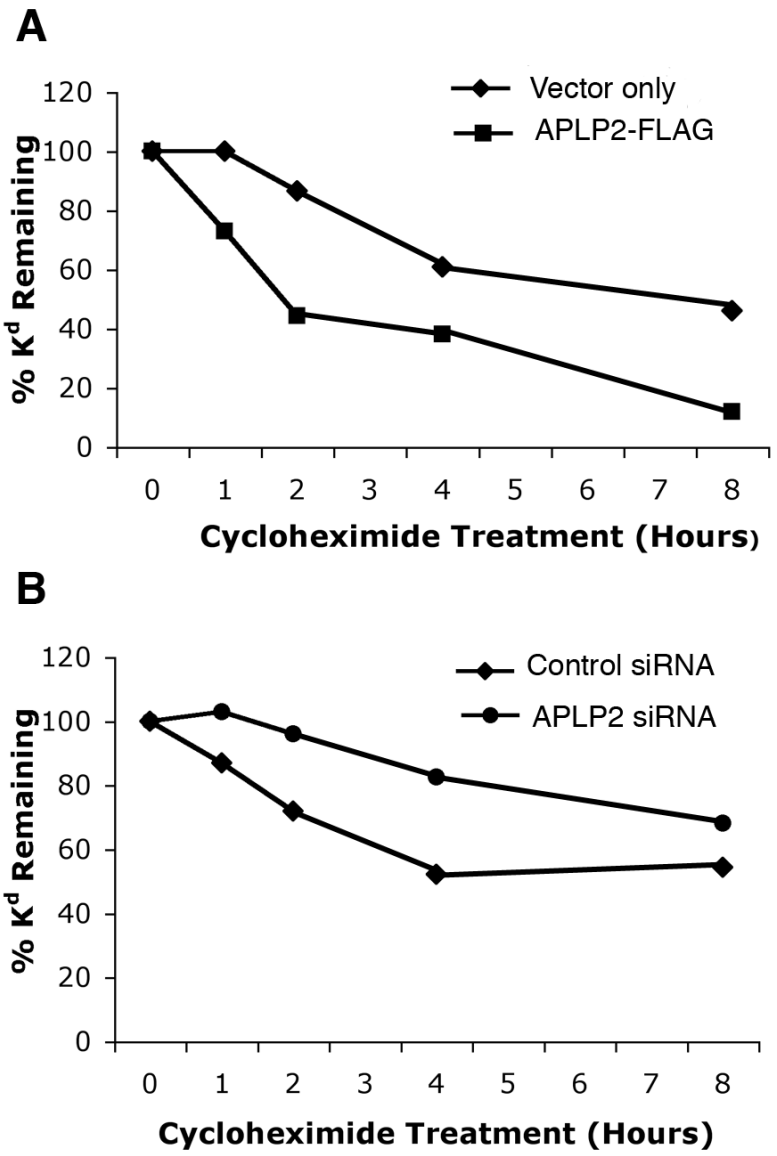

Figure 7.

K^d turnover was augmented as a result of increased APLP2 expression. HeLa-etK^d cells (stably expressing K^d) were transiently transfected with (*A*) the pCMVTag4A vector (■) or FLAG-tagged APLP2 in pCMVTag4A (◆) or (*B*) APLP2 siRNA (●) or control siRNA (◆). After 48 h of transfection, the cells were treated with 10 μg/ml cycloheximide for 0, 1, 2, 4, or 8 hours. Equivalent numbers of live cells from each time point were lysed and centrifuged, and samples of the supernatants were boiled, electrophoresed, transferred to Western blots, and probed with the 64-3-7 Ab that recognizes denatured epitope-tagged K^d (Ab 64-3-7) or with an Ab that recognizes β-actin. The band intensity for K^d was normalized to the β-actin band intensity at the corresponding time point. Values are shown on the graph for the percentage of remaining K^d at the 0-, 1-, 2-, 4-, and 8-h time points.